Indian Journal of Veterinary Anatomy 37(1): 4-11, June 2025

Histological, Histochemical, and Scanning Electron-Microscopical Studies on the Vestibular Region of Nasal Cavity in Dogs

Shikha Saini[1] and Pawan Kumar[2*]
Department of Veterinary Anatomy, College of Veterinary Sciences
Lala Lajpat Rai University of Veterinary and Animal Sciences, Hisar-125004, India

Received: 25 June 2025; Accepted: 15 July 2025

ABSTRACT

The present study was conducted to determine the histological, histochemical, and scanning electron-microscopical details of the vestibular region of the nasal cavity in adult dogs. The mucosa of the vestibular region (straight and the alar folds, and rostral portions of the dorsal and ventral nasal turbinates) was lined by a non-keratinized stratified squamous epithelium. The superficial part of the propria submucosa contained different connective tissue cells, collagen, elastic, and reticular fibres in various concentrations, isolated sero-mucous glands, fine blood capillaries, small blood vessels, and venous caverns-like structures. The deeper portion featured large clusters of sero-mucous glandular acini along with their ducts, nerve bundles, and blood vessels. Hyaline cartilage in the deeper part formed a supportive framework. The stratified squamous lining, gradually transitioned caudally into stratified cuboidal (transitional zone) to pseudostratified columnar type with occasional goblet cells. The glandular units reacted differently to various histochemical stains revealing different moieties of carbohydrates but these glands were lacking proteins in their secretions. SEM presented small, irregular, scale-like flat squamous cells which were continuous with each other, displaying microplicae in various arrangements at higher magnification. In the region of transition, a few ciliated cells started appearing along with some raised cells bearing microvilli of different shapes and sizes and a few goblet cells.

Keywords: Vestibule, Alar fold, Straight fold, Dogs, Scanning electron-microscopy

INTRODUCTION

The nasal cavity plays a crucial role in preparing inhaled air by adjusting its temperature and humidity, enabling the sense of smell, and filtering out suspended particles and droplets (Kumar *et al*., 2000). The nasal cavity is divided into three distinct regions: the vestibular, respiratory, and olfactory areas, each specialized for a specific primary function that sets it apart from the others (Yang *et al*., 2017). The warming and humidification of inhaled air start in the nasal vestibule and continue along the airway mucosa towards the posterior side. Most of this conditioning takes place in the rostral part of the nasal cavity (Blatt *et al*., 1972; Scott, 1954; Walker *et al*., 1961). Magilton and Swift (1968) identified two countercurrent heat exchange mechanisms in dogs: an external mechanism involving heat transfer between the venous lake in the alar fold of the nasal vestibule and the surrounding air, and an internal mechanism involving heat exchange between venous blood in the cavernous sinus and warm arterial blood within the carotid rete thus, describing prime role of alar fold region. The nasal cavity serves as the primary entry point for numerous respiratory illnesses, including influenza and pneumonia, making it a vital component of the body's defense system (Qin *et al*., 2015; Tomosada *et al*., 2013). Functional and behavioral research has shown that dogs possess a superior sense of smell compared to many other mammalian species, allowing them to detect extremely low concentrations of scent molecules and differentiate between the odours of individual beings (Hafez, 1962; Bradshaw, 1992). However, little has been reported concerning the morphological and structural details of the vestibular portion of nasal cavity. Hence, the current study focuses on the histology and scanning electron-microscopy of the nasal vestibule.

MATERIALS AND METHODS

The present study was conducted on 10 adult, local, non-descript dogs. The heads were procured from the Department of VCC, LUVAS, Hisar immediately after the death of the animals. Six heads used for histological and histochemical studies were fixed in 10% neutral buffered formalin solution for 48 hours and then, sectioned into mid sagittal and transverse planes. The tissues were collected from

1. Ph.D. Student; 2. Professor

*Corresponding Author: E-mail: pkumar@luvas.edu.in

straight and alar folds and rostral portions of the dorsal and ventral nasal turbinates. The fixed tissues were processed for routine paraffin technique for light microscopy (Luna, 1968). The paraffin sections of 5-6 µ were cut and stained with various stains: Routine Harris' haematoxylin and eosin stain for general architecture (Luna, 1968), Gomori's method for reticular fibres (Luna, 1968), Weigert's method for elastic fibres (Luna, 1968), Crossmon's trichrome stain for collagen fibres (Crossmon, 1937), Ayoub-Shklar's method for keratin and prekeratin (Luna, 1968), McManus' method for glycogen (PAS) (Luna, 1968), Alcian blue method for mucosubstances (pH 2.5) (Luna, 1968), PAS-Alcian blue method for acidic and neutral mucopolysaccharides (pH 2.5) (Luna, 1968), Mayer's mucicarmine method for mucin (Luna, 1968), colloidal iron method for acid mucopolysaccharides (Luna, 1968), mercury bromphenol blue method for proteins (Pearse, 1968), and performic acid Alcian blue method for proteins (Pearse, 1968).

Selected fresh tissues from the remaining heads were collected and fixed in 2% glutaraldehyde solution for 6-8 hours after thorough washing in chilled 0.1 M phosphate buffer (pH 7.4). The tissues were rewashed twice with phosphate buffer and rest of the procedure was carried out at EM Lab., AIIMS, New Delhi. The tissues were dehydrated in ascending grades of alcohol, critical point dried, mounted on stubs and then, sputter coated with gold. Lastly, the processed tissues were viewed under scanning electron microscope to record observations and areas of interest were photographed using Zeiss EVO18 and Apreo 2S microscopes.

RESULTS AND DISCUSSION

The present study elucidated that the mucosa of vestibular region of the nasal cavity was lined by a non-keratinized stratified squamous epithelium (Figs. 1-4) as reported earlier in Iraqi goat (Mustafa and Reshag, 2018), pig (Larochelle and Martineau-Doize, 1990; Kalita, 2014; Parkash and Kumar, 2019), Bama minipig (Yang *et al*., 2017), sheep (Ganganaik *et al*., 2007; Ganganaik *et al*., 2009), goat (Kumar *et al*., 1992; Kumar *et al*., 1999), dog (Adams and Hotchkiss, 1983; Kumar *et al*., 1994), and camel (Suman *et al*., 1998; Badawi and El-Bab, 1974). On the contrary, a thick keratinized stratified squamous epithelial covering had been documented in Gaddi sheep, goat, pig, and dog (Pathak and Rajput, 2018; Kahwa and Purton, 1996; Manjunatha *et al*., 2018; El-Bakary *et al*., 2019; Al-kafagy and Reshag, 2020). However, the epithelium was identified as keratinized stratified squamous in the cranial region, gradually transitioning to a non-keratinized form towards the caudal portion in camel (Gewaily *et al*., 2019; Abdel-Salam *et al*., 2014). Whereas, a stratified cuboidal epithelium lined this region in cattle (Adams, 1986), buffalo (Kumar *et al*., 2008), and horse (Kumar *et al*., 2000). Girgiri *et al*. (2022) noted that the lining epithelium of alar fold was stratified squamous non-keratinized and that of the straight fold was stratified squamous slightly keratinized in Yankasa sheep. The free surface of the epithelium had an undulating appearance, while the deeper surface or the basal stratum exhibited papillary pegs of varying shapes and sizes (Figs. 1-3). These features were in accordance with observations in other domestic animals like Iraqi goat (Mustafa and Reshag, 2018), dog (Dellmann, 1993; Kumar *et al*., 1994; El-Bakary *et al*., 2019), pig (Manjunatha *et al*., 2018; Parkash and Kumar, 2019), Yankasa sheep (Girgiri *et al*., 2022), goat (Kumar *et al*., 1992), and camel (Badawi and El-Bab, 1974; Suman *et al*., 1998).

The stratum basale was comprised of a single layer of columnar cells with oval nuclei, being oriented perpendicular to the epithelium towards the basal portion. In between these cells, lymphoid cells of different origins were also interspersed. Abdel-Salam *et al*. (2014) also mentioned that migratory lymphocytes and mast cells were often seen in the basal layer of the epithelium in camels. Melanocytes were also noticed between the basale cells in the initial portions of the alar fold however, these cells disappeared caudally. The stratum spinosum cells presented a similar pattern of nuclei in the deeper layers to those of the stratum basale, though these nuclei were larger in dimensions. The superficial layers of the stratum spinosum contained round to oval, larger nuclei. These cells presented a spicule-like arrangement with more eosinophilic cytoplasm. The stratum superficiale cells were the largest having round to oval nuclei which were generally horizontally placed. The cytoplasm of these cells was finely granular and eosinophilic. The outermost layer was comprised of a single layer of flattened squamous cells. Their nuclei were small, rod-like and deeply basophilic as they were showing some degenerative changes. The cytoplasm of these cells was strongly eosinophilic in nature.

The subepithelial part of the propria submucosa was having loose irregular connective tissue which was in agreement with the studies of Kumar *et al*. (1992) in goat, Kumar *et al*. (2000) in horse, Parkash and Kumar (2019) in pig, Girgiri *et al*. (2022) in Yankasa sheep, Ganganaik *et al*. (2009) and Pathak and Rajput (2018) in sheep, with isolated sero-mucous glands (Fig. 2). In contrast, the propria submucosa consisted of dense irregular fibrous connective tissue in Iraqi goat (Mustafa and Reshag, 2018), camel (Gewaily *et al*., 2019), and dog (El-Bakary *et al*., 2019; Al-kafagy and Reshag, 2020). The reticular fibres formed a mesh-like network beneath the epithelium, particularly in the connective tissue which alternated with the epithelial rete pegs and contributed to the formation of the basement membrane. The superficial propria submucosa contained different connective tissue cells, few lymphoid cells, collagen, elastic, and reticular fibres in various concentrations (Fig. 4), isolated sero-mucous glands, fine blood capillaries, blood vessels, and venous cavern-like structures (Figs. 1-3).

The deeper portion of the propria submucosa was constituted by large clusters of sero-mucous glandular acini, nerves, and blood vessels of various thickness (Fig. 5) as also observed in camel (Badawi and El-Bab, 1974; Gewaily *et al*., 2019), sheep (Ganganaik *et al*., 2009; Pathak and Rajput, 2018), pig (Manjunatha *et al*., 2018), and dog (El-Bakary *et al*., 2019). However, this region housed sero-mucous glands, with serous acini being more predominant in pig (Kalita, 2014; Parkash and Kumar, 2019) and sheep (Khamas and Ghoshal, 1982). On the contrary, the serous glands were organized into superficial and deep layers within the propria in horse (Kumar *et al*., 2000), camel (Abdel-Salam *et al*., 2014), and goat (Kumar *et al*., 1992; Kahwa and Purton, 1996; Mustafa and Reshag, 2018) whereas, mucous vestibular glands were recorded in dogs (Al-kafagy and Reshag, 2020). Clusters of glandular acini, arranged in lobules have also been observed in Yankasa sheep (Girgiri *et al*., 2022). Similarly, Kahwa and Purton (1996) in goats revealed that the orifices of submucosal glands were abundant in the rostral regions of the nasal cavity. Dense collagen bundles were oriented in various directions in the deeper portions, especially around the glandular acini, blood vessels and venous caverns as also noted in horse (Kumar *et al*., 2000), sheep (Ganganaik *et al*., 2009), and pig (Parkash and Kumar, 2019). Randomly oriented elastic fibers were more concentrated in the deeper areas. Reticular fibres encased the individual glandular acini as well as the glandular clusters and were seen distributed around blood vessels and nerve bundles, aligning with the reports of Manjunatha *et al*. (2018) in pig.

The intra and inter glandular ducts associated with these glands were lined with simple cuboidal epithelium as documented earlier by Kumar *et al*. (1992) in goats, except for a few ducts which had stratified cuboidal epithelium with wide lumens (Fig. 5) and these ducts extended superficially to open onto the free surface of the epithelium. In horse, these ducts were lined with simple cuboidal to low columnar epithelium (Kumar *et al*., 2000) whereas, in camels, Gewaily *et al*. (2019) mentioned that the ducts were initially lined with simple columnar epithelium, transitioning to pseudostratified epithelium at the surface where these ducts opened. Large blood capillaries and venous cavern-like structures were observed, along with a few nerve bundles. The venous caverns were thin-walled structures with a valve-like arrangement in their walls, which may help regulate blood flow (Fig. 3). Some of them were very large in size and contained RBCs in their lumen. Additionally, blood vessels of various shapes and sizes were present, including some exceptionally large vessels. A hyaline cartilage was embedded in the deeper regions which supported the propria submucosa corroborating with the studies of Parkash and Kumar (2019) in pig, Ganganaik *et al*. (2009) in sheep, Gewaily *et al*. (2019) in camel, and Girgiri *et al*. (2022) in Yankasa sheep. Dense arrangement of collagen fibres surrounding the cartilage forming the perichondrium were also observed.

A positive reaction was observed revealing the presence of glycogen in the sero-mucous glands with mucous type being dominant, while no activity was detected in the ducts (Fig. 6). The hyaline cartilage showed a strong positive reaction to McManus' PAS stain. The combined PAS-Alcian blue method revealed the predominance of neutral mucopolysaccharides in the glands, while the ducts showed no affinity (Fig. 7). Likewise, the glandular units in camels exhibited a strong reaction to both PAS and the PAS-Alcian blue combination (Abdel-Salam *et al*., 2014). The glandular clusters did not show Alcianophilic reactions but a strong affinity was noted in the hyaline cartilage. On the contrary, these adenomeres showed a positive reaction to the

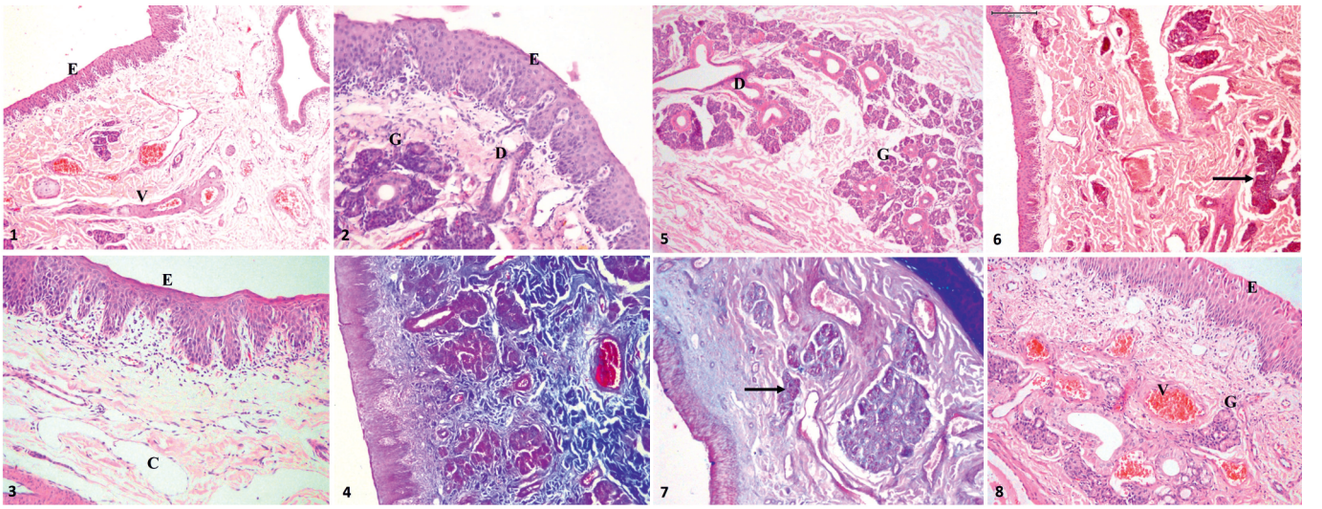

Photomicrograph showing **Fig. 1:** Stratified squamous non-keratinized epithelium (E) of straight fold. H. & E. x 100; **Fig. 2:** Dorsal nasal turbinate. H. & E. x 200; **Fig. 3:** Rostral portion of ventral nasal turbinate. H. & E. x 100. Note blood vessels (V), glands (G), venous caverns (C) and duct (D); **Fig. 4:** Collagen fibres (blue colour) in the propria submucosa. Crossmon's trichrome method x 100.
Photomicrograph showing glands (G) and their ducts (D) in propria submucosa **Fig. 5:** Alar fold. H. & E. x 100; **Fig. 6:** Straight fold-glycogen (arrow). McManus' PAS method x 100; **Fig. 7:** Alar fold - Predominance of neutral mucopolysaccharides (arrow). PAS-Alcian blue method x 100; **Fig. 8:** Rostral portion of ventral nasal turbinate. H. & E. x 100. Note transition of epithelium into respiratory type (E) along with glands (G) and blood vessels (V).

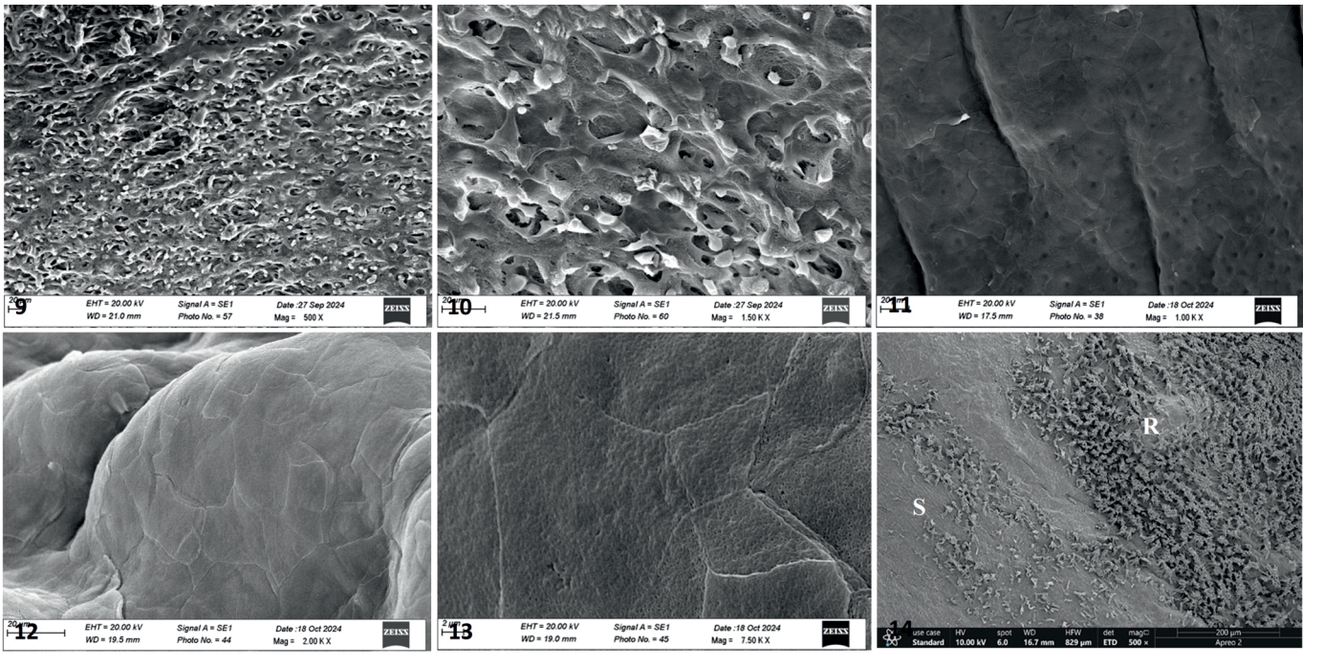

Scanning electron-micrograph showing **Fig. 9:** Plaques-like arrangement of cells in straight fold. x 500; **Fig. 10:** Different cells and openings of ducts in rostral portion of DNT. x 1500; **Fig. 11:** Longitudinal grooves and their polyangular cells with central depressions of alar fold. x 1000; **Fig. 12:** Presence of flat cells on the surface of undulating folds of alar fold. x 2000; **Fig. 13:** Flat cells at higher magnification showing microplicae system. x 7500; **Fig. 14:** Transition of stratified squamous (S) and respiratory regions (R). x 500.

Alcian blue stain in camel (Abdel-Salam *et al*., 2014). The glands were devoid of any activity indicating the absence of mucins by the Mayer's mucicarmine method. The colloidal iron method demonstrated very weak positive reaction. The performic acid-Alcian blue method demonstrated no reaction in the glandular acini but a mild reaction was noticed in the cartilage. However, Parkash and Kumar (2019) reported that the mucous acini showed positive reaction for glycogen, sialomucins, hyaluronic acid, weakly sulfated acidic mucosubstances, acidic, neutral mucopolysaccharides, and proteins.

The current study showed that the lining epithelium

in the vestibular region i.e., stratified squamous non-keratinized epithelium, gradually transitioned caudally into stratified cuboidal (transitional zone) to pseudostratified columnar type with occasional goblet cells (Fig. 8). Such observations go parallel with the findings in domestic animals (Dellmann, 1993), Bama minipigs (Yang *et al*., 2017), pigs (Parkash and Kumar, 2019; Manjunatha *et al*., 2018; Larochelle and Martineau-Doize, 1990), camels (Abdel-Salam *et al*., 2014; Gewaily *et al*., 2019), laboratory animals, dogs, and non-human primates (Chamanza and Wright, 2015), bovines (Adams, 1986), goats (Kumar *et al*., 1992; Kahwa and Purton, 1996), and dogs (Adams and Hotchkiss, 1983). However, in Yankasa sheep, the rostral two-thirds of the ventral nasal turbinate exhibited this transition zone (Girgiri *et al*., 2022). Similarly, a transition zone showing stratified columnar epithelium was noticed in Iraqi goats (Mustafa and Reshag, 2018).

The stratified cuboidal epithelium exhibited elongated, narrow, vertically oriented nuclei in the cells which were closer to the basement membrane. These nuclei were basophilic, generally with centered nucleoli. Adjacent 2 to 3 rows of nuclei also had similar features. The nuclei of the next superficial 2-3 layers were having round to oval nuclei and distinct nucleoli. The cytoplasm of these cells was finely granular and eosinophilic, with the eosinophilia becoming more pronounced as progressed towards the surface. The most superficial cells were cuboidal in shape with densely basophilic nuclei, and the nucleoli were typically not visible. The cytoplasm of these cells was more eosinophilic compared to the deeper cells. The free surface of the epithelium did not show any cilia. In addition to this, lymphoid cells infiltrated the epithelium at various levels. The deepest surface of the epithelium displayed narrow epithelial pegs. A few goblet cells which were intensely PAS positive also started appearing in between the epithelial cells when stained with McManus' PAS method. The combined PAS-Alcian blue method revealed that the goblet cells were strongly positive indicating a predominance of acidic mucopolysaccharides. The Mayer's mucicarmine and colloidal iron methods showed that the goblet cells lacked mucins and acidic mucopolysaccharides, respectively. Additionally, the goblet cells exhibited no affinity for the performic acid-Alcian blue method indicating the absence of more than 4% cysteine in their contents. At some places, a pseudostratified appearance of the epithelium was also observed. The rest of the histological and histochemical features were similar as described earlier.

SEM of the vestibular region presented small, irregular plaque-like structures in the regions of straight fold and rostral portions of the dorsal and ventral nasal turbinates (Figs. 9, 10) whereas, scale-like flat cells in the alar fold region (Figs. 11, 12). These cells represented the squamous cells which varied in shapes and sizes and were continuous with each other. However, the rostral section of the nasal vestibule displayed polyangular squamous cells of different sizes in goat (Kahwa and Balemba, 1998; Kumar *et al*., 1999), horse (Kumar *et al*., 2000), and camel (Abdel-Salam *et al*., 2014; Gewaily *et al*., 2019). In buffalo calves (Kumar *et al*., 2008) and pigs (Parkash *et al*., 2019), polyangular cells with prominently convex surfaces that appeared to bulge outward from the surface were noted. Ganganaik *et al*. (2007) observed flat, leaf-shaped cells in sheep. The junctions between adjacent cells were distinctly visible in the region of alar fold (Figs. 11, 12), but not clear in other regions. However, linear depressions separated the borders of neighboring epithelial cells in goat (Kumar *et al*., 1999), horse (Kumar *et al*., 2000), sheep (Ganganaik *et al*., 2007), and camel (Abdel-Salam *et al*., 2014; Gewaily *et al*., 2019). Many exfoliated cells were also present over the surface which stands similar to the observations of Kahwa and Balemba (1998) in goat and Ganganaik *et al*. (2007) in sheep.

The flat squamous cells in the region of longitudinal grooves of alar fold displayed shallow depressions with microplicae in various arrangements at higher magnification. However, in other regions microplicae were observed but the depressions were lacking (Fig. 13). This presence of microplicae patterns was consistent with observations in goat (Kahwa and Balemba, 1998; Kumar *et al*., 1999) and sheep (Ganganaik *et al*., 2007). Conversely, microplicae were absent in buffalo calves (Kumar *et al*., 2008). However, small microvilli were noted on the surface of these cells in horse (Kumar *et al*., 2000), buffalo calves (Kumar *et al*., 2008), goat (Kahwa and Balemba, 1998), camel (Abdel-Salam *et al*., 2014; Gewaily *et al*., 2019), and pig (Parkash *et al*., 2019). In the caudal portion of the vestibule, the cells displayed a wave-like arrangement and further caudally, towards the vestibular end, squamous cells were non-keratinized and, in some cases, exhibited microridges in camel (Abdel-Salam

et al., 2014; Gewaily *et al*., 2019). In between the squamous cells, large openings of ducts were observed (Fig. 10), similar to the findings in buffalo (Kumar *et al*., 2008) and goat (Kahwa and Balemba, 1998). In camels, duct openings were particularly noted at the junction between the mucous and cutaneous regions of the nasal vestibule (Abdel-Salam *et al*., 2014; Gewaily *et al*., 2019).

Towards the caudal portion of the vestibular region, a transition zone showing transformation of stratified squamous epithelium into pseudostratified ciliated columnar epithelium was observed (Fig. 14), as seen in goats (Kumar *et al*., 1999), sheep (Ganganaik *et al*., 2007), buffalo calves (Kumar *et al*., 2008), and dogs (Adams and Hotchkiss, 1983). In this region, a few ciliated cells started appearing between the adjacent squamous cells along with some raised cells with microvilli of different shapes and sizes (Fig. 14). The appearance of patches of ciliated cells indicated the transition from the vestibular to the respiratory region in cattle (Adams, 1986), horse (Kumar *et al*., 2000), goat (Kumar *et al*., 1999), and pig (Parkash *et al*., 2019). In goats (Kumar *et al*., 1999; Kahwa and Balemba, 1998) and buffalo calves (Kumar *et al*., 2008), only a few ciliated cells with short, irregular cilia were noted. Among the ciliated cells, microvillus cells with small microvilli were interspersed in bovines (Adams, 1986), horse (Kumar *et al*., 2000), goat (Kumar *et al*., 1999), buffalo calves (Kumar *et al*., 2008), and pig (Parkash *et al*., 2019). Additionally, cells bearing long microvilli were observed in both camels (Gewaily *et al*., 2019) and pigs (Parkash *et al*., 2019). At places, a few cells resembling goblet cells were also noted along with the openings of ducts of varying shapes and sizes which align with the findings of Adams (1986) in cattle and Kumar *et al*. (2008) in buffalo calves. In goats, Kahwa and Balemba (1998) reported mucous-secreting cells with apical protuberances and submucosal glandular openings in aboral-most region of vestibule. The region was caudally followed by ciliated zone having microvillus and ciliated cells.

REFERENCES

Abdel-Salam, L.R., Hussein, S.A., Gad, M.H., Khattal, A.A.A. and Amer, A.H. 2014. Histological, histochemical and scanning electron microscopical study of nasal cavity epithelium of the dromedary camel *(Camelus dromedarius)*. *Journal of Basic Medical and Allied Sciences* 2 : 1-24.

Adams, D.R. 1986. Transitional epithelial zone of the bovine nasal mucosa. *The American Journal of Anatomy* 176 : 159-170.

Adams, D.R. and Hotchkiss, D.K. 1983. The canine nasal mucosa. *Anatomia Histologia Embryologia* 12 : 109-125.

Al-Kafagy, S.M., and Reshag, A.F. 2020. Histological features of the nasal cavity in indigenous dogs. *Plant Archives* 20 : 7979-7984.

Badawi, H. and El-Bab, M.R.F. 1974. Anatomical and histological studies on the nasal cavity of the camel (*Camelus dromedarius*). *Assiut Veterinary Medical Journal* 1 : 1-14.

Blatt, C.M., Taylor, C.R., and Habal, M.B. 1972. Thermal panting in dogs: the lateral nasal gland, a source of water for evaporative cooling. *Science* 177 : 804-805.

Bradshaw, J.W.S. 1992. *The Waltham Book of Dog and Cat Behavior*. pp. 31-52. Thorne, C. (Edt.), Pergamon Press, Oxford.

Chamanza, R., and Wright, J.A. 2015. A review of the comparative anatomy, histology, physiology and pathology of the nasal cavity of rats, mice, dogs and non-human primates. Relevance to inhalation toxicology and human health risk assessment. *Journal of Comparative Pathology* 153 : 287-314.

Crossmon, G. 1937. A modification of Mallory's connective tissue stain with a discussion of principles involved. *The Anatomical Record* 69 : 33-38.

Dellmann, H.D. 1993. *Textbook of Veterinary Histology*. 4th edn., Lea and Febiger, Philadelphia, USA.

El-Bakary, R., Enany, E.S.E., Karkoura, A.A., Abumandour, M., and Gafaar, S.F. 2019. Histological characterizations of the nasal conchae of the dog (*Canis lupus*). *Alexandria Journal of Veterinary Sciences* 60 : 42-47.

Ganganaik, S., Jain, R.K. and Kumar, P. 2009. Histological studies on the nasal cavity of sheep (*Ovis aries*). *Haryana Veterinarian* 48 : 68-71.

Ganganaik, S., Jain, R.K., Kumar, P. and Gupta A.N. 2007. Scanning electron microscopic studies

on the nasal cavity of sheep (*Ovis aries*). *Indian Journal of Animal Sciences* 77 : 878-879.

Gewaily, M., Hadad, S., and Shoghy, K. 2019. Gross, histological and scanning electron morphological studies on the nasal turbinates of one humped camel (*Camelus dromedarius*). *Bioscience Research* 16 : 107-120.

Girgiri, I.A., Malah, M.K., Jiji, M.H. and Gazali, Y.A. 2022. Gross and histological studies of the nasal turbinates in Yankasa sheep (*Ovis aries*) in Maiduguri, Nigeria. *Sahel Journal of Veterinary Sciences* 19 : 13-20.

Hafez, E.S.E. 1962. *The Behavior of Domestic Animals*. 1st edn., Bailliere Tindall and Cox, London.

Kahwa, C.K.B. and Balemba, O.B. 1998. The non-olfactory nasal epithelium in the adult goat: a scanning electron microscopic study. *Small Ruminant Research* 29 : 277-282.

Kahwa, C.K.B. and Purton, M. 1996. Histological and histochemical study of epithelial lining of the respiratory tract in adult goats. *Small Ruminant Research* 20 : 181-186.

Kalita, A. 2014. Histomorphological study of the respiratory system of Mizo local pig (*Zo Vawk*). *Asian Journal of Biomedical and Pharmaceutical Sciences* 4 : 50-54.

Khamas, W.A.H. and Ghoshal, N.G. 1982. Histomorphologic studies of the nasal cavity of sheep (*Ovis aries*) and its significance in temperature regulation of the brain. *Acta Anatomica* 113 : 340-351.

Kumar, P., Timoney, J.F., Southgate, H.H.P. and Sheoran, A.S. 2000. Light and scanning electron microscopic studies of the nasal turbinates of the horse. *Anatomia Histologia Embryologia* 29 : 103-109.

Kumar, Pawan, Gupta, A.N., and Nagpal, S.K. 2008. Scanning electron microscopy of the nasal cavity of the buffalo calves (*Bubalus bubalis*). *Indian Journal of Animal Sciences* 78 : 1094-1097.

Kumar, Pawan, Kumar, S. and Singh, Y. 1992. Histological studies on the nasal turbinates of goat. *Indian Journal of Animal Sciences* 4 : 75-79.

Kumar, Pawan, Kumar, S. and Singh, Y. 1994. Histology of nasal turbinates in dog. *Indian Journal of Animal Sciences* 64 : 1050-1053.

Kumar, Pawan, Kumar, S. and Singh, Y. 1999. Scanning electron-microscopic studies on the nasal cavity of goat. *Indian Journal of Animal Sciences* 69 : 887-890.

Larochelle, R., and Martineau-Doize, B. 1990. Distribution of epithelia in the nasal cavity of piglets. *Acta Anatomica* 139 : 214-219.

Luna, L.G. 1968. *Manual of Histologic Staining Methods of Armed Forces Institute of Pathology.* 3rd edn., McGraw Hill Book Co., New York.

Magilton, J.H., and Swift, C.S. 1968. Description of two physiological heat exchange systems for the control of brain temperature. *IEEE Conference Record: Annual Rocky Mountain Bioengineering Symposium* 5 : 24-27.

Manjunatha, K., Jamuna, K.V., Parsad, R.V., Naryanaswamy, H.D., Sanganal, J.S., and Girish, M.H. 2018. Histological study of nasal cavity in pigs. *International Journal of Chemical Studies* 6 : 1658-1660.

Mustafa, A.R., and Reshag, A.F. 2018. Histological study on the nasal cavity of black Iraqi goat (*Capra hircus*). *The Iraqi Journal of Veterinary Medicine* 42 : 105-111.

Parkash, T., and Kumar, Pawan. 2019. Histological and histochemical studies on the nasal cavity of the young pigs (*Sus scrofa*). *Indian Journal of Veterinary Anatomy* 31 : 40-43.

Pathak, V., and Rajput, R. 2018. Histological and histochemical studies on the nasal cavity of Gaddi sheep. *Indian Journal of Small Ruminants* 24 : 281-287.

Pearse, A.G.E. 1968. *Histochemistry*: *Theoretical and Applied*. 3rd edn., Vol. 2. Churchill Livingstone, London.

Qin, T., Yin, Y., Huang, L., Yu, Q. and Yang, Q. 2015. H9N2 influenza whole inactivated virus combined with polyethyleneimine strongly enhances mucosal and systemic immunity after intranasal immunization in mice. *Clinical and Vaccine Immunology* 22 : 421-429.

Scott, J.H. 1954. Heat regulating function of the nasal mucous membrane. *The Journal of Laryngology & Otology* 68 : 308-317.

Suman, Singh, G. and Nagpal, S.K. 1998. Histological studies on the nasal cavity of Indian camel (*Camelus dromedarius*). *Journal of Camel Practice and Research* 5 : 99-104.

Tomosada, Y., Chiba, E., Zelaya, H., Takahashi, T., Tsukida, K. and Kitazawa, H. 2013. Nasally administered Lactobacillus rhamnosus strains differentially modulate respiratory antiviral immune responses and induce protection against respiratory syncytial virus infection. *BMC immunology* 14 : 1-16.

Walker, J.E.C., Wells Jr, R.E. and Merrill, E.W. 1961. Heat and water exchange in the respiratory tract. *The American Journal of Medicine* 30 : 259-267.

Yang, J., Dai, L., Yu, Q. and Yang, Q. 2017. Histological and anatomical structure of the nasal cavity of Bama minipigs. *PLoS One* 12 : 1-14.